Gap-Inhomogeneity-Induced Electronic States in Superconducting $Bi_2Sr_2CaCu_2O_{8+\delta}$

A. C. Fang,[1] L. Capriotti,[2] D. J. Scalapino,[3] S. A. Kivelson,[4] N. Kaneko,[5,*] M. Greven,[1,5] and A. Kapitulnik[1,4]

[1]*Department of Applied Physics, Stanford University, Stanford, California 94305, USA*
[2]*Credit Suisse First Boston, Ltd. (Europe), One Cabot Square, London E14 4QJ, United Kingdom*
[3]*Department of Physics, University of California, Santa Barbara, California 93106-9530, USA*
[4]*Department of Physics, Stanford University, Stanford, California 94305, USA*
[5]*Stanford Synchrotron Radiation Laboratory, Stanford, California 94309, USA*

(Received 10 August 2005; published 12 January 2006)

In this Letter, we analyze, using scanning tunneling spectroscopy, the density of electronic states in nearly optimally doped $Bi_2Sr_2CaCu_2O_{8+\delta}$ in zero magnetic field. Focusing on the superconducting gap, we find patches of what appear to be two different phases in a background of some average gap, one with a relatively small gap and sharp large coherence peaks and one characterized by a large gap with broad weak coherence peaks. We compare these spectra with calculations of the local density of states for a simple phenomenological model in which a $2\xi_0 \times 2\xi_0$ patch with an enhanced or suppressed d-wave gap amplitude is embedded in a region with a uniform average d-wave gap.

DOI: 10.1103/PhysRevLett.96.017007 PACS numbers: 74.72.Hs, 74.25.−q, 74.50.+r

One of the surprising features revealed by scanning tunneling microscopy (STM) studies of the high T_c superconductor $Bi_2Sr_2CaCu_2O_{8+\delta}$ (BSCCO) is a pattern of patches of what appear to be two different phases, with significant differences in their electronic structures [1–6]. There are regions of a relatively small local gap, $\Delta(\vec{r}) \sim$ 25–35 meV, in which the peak in the local density of states (LDOS) at $V = \Delta$ is relatively sharp in energy and the peak height is very large. Other regions have a larger gap, with $\Delta(\vec{r}) \sim$ 50–75 meV, and broad and small peaks (see Fig. 1). It is tempting (as is widely assumed) to associate these very different electronic structures with two different bulk electronic phases: the small-gap regions, because they appear to have distinct coherence peaks, are identified as regions of ''good'' superconductivity, whereas the large-gap regions are like a pseudogap phase which competes with superconductivity. This latter identification found support from data suggesting that there is a subtle form of local charge-density wave order with period near four lattice constants (''stripes'' or ''checkerboards'') [5–11] which is most apparent in the large-gap regions [5,10]. However, because the characteristic size of the regions ($L \simeq 30$ Å) is not much larger than the superconducting coherence length ($\xi_0 \sim$ 15–20 Å), it is clear that whatever the bulk character of each region, superconducting correlations can leak from one region into the other via the proximity effect [2], thus complicating any such identification.

In this Letter, we report results of STM studies on nearly optimally doped $Bi_2Sr_2CaCu_2O_{8+\delta}$ [12] with high spatial and fine energy resolution. From these improved data, we observe, as illustrated in Fig. 1, the following: (1) In the small-gap regions, the peaks in the LDOS are too large to be the coherence peaks of a uniform BCS d-wave superconductor [see Fig. 1(a)]; there is excessive spectral weight compared to the number of states pushed up from below the gap. (2) The peaks in the large-gap regions are too broad and small to be the coherence peaks of a uniform BCS d-wave superconductor [see Fig. 1(c)]. (3) These regions are interspersed in a background ''average'' gap $\bar{\Delta} \equiv \Delta_0 \approx 40$ meV that produces a visible feature (typically, a shoulder) in the LDOS in nearby regions; this coincides with the gap inferred from angle resolved photoemission measurements [14,15].

To interpret these results, we have calculated the quasiparticle LDOS for a mean-field d-wave BCS model in which the strength of the pairing field (gap amplitude) is changed in a small $L \times L$ patch with $L \sim 2\xi_0$. We find

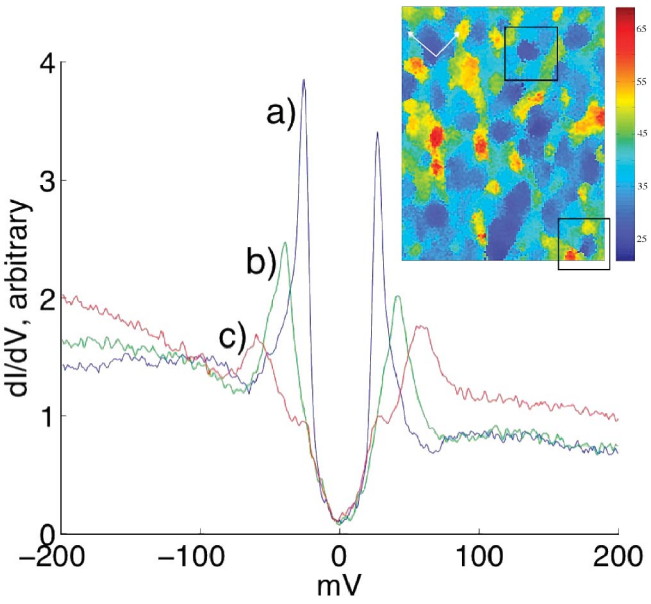

FIG. 1 (color). Example spectra in a (a) small-, (b) average-, and (c) large-gap region. Inset is a typical 220 Å × 280 Å map of gap size. Crystal axes and squares that relate to Fig. 2 are marked.

that structure like that seen in the "small-gap regions" arises from resonant bound states if the gap amplitude vanishes (or is, at least, small compared to the peak energy) in the $L \times L$ patch [see Fig. 3(b)]. A structure similar to that seen in the large-gap regions is found if a large pairing field is assumed inside such a patch [16] [see Fig. 3(c)]. One is thus led to conclude that small-gap regions with "large coherence peaks" are regions with a much smaller than average pairing potential. Conversely, the fact that the concentration of large-gap regions increases in increasingly underdoped samples suggests that these regions, despite their strong pairing tendencies, have little or no superfluid density (phase stiffness) [17]. Finally, the fact that we see spectral features "leaking" between regions suggests that we are seeing patches of proximity coupled phases.

For tunneling perpendicular to the Cu-O planes, a typical d-wave BCS shape of the spectrum is expected, characterized by a "v-shaped" LDOS at low bias and coherence peaks that accommodate the spectral weight from the opening of a gap with nodes. Early on, the general d-wave shape of STM spectra was confirmed in BSSCO [18]; however, data always appeared with significant particle-hole asymmetry in the background and subsequent analyses revealed that very few spectra quantitatively fit a BCS d-wave prediction, especially the coherence peak strength and shape.

Figure 1 shows spectra often seen in the small-, average-, and large-gap regions. In our analysis, we define the (positive bias) peak energy in the LDOS as the local gap $\Delta(\vec{r})$. In our samples, we find that the average gap is $\Delta_0 \sim 40$ meV [2,5,6,9] and that approximately 75% of the area has a gap that is within ± 10 meV of the average. This region surrounds patches of smaller gap ($\Delta \leq 30$ meV, cover $\sim$15% of the area) and patches of larger gap ($\Delta \geq 50$ meV, covering $\sim$10%). We also note that although the differences between spectra are more subtle at energies far below the gap [2,4], the shape between the two coherence peaks tends to be more v-shaped in the large- and average-gap regions, and more rounded where the coherence peaks are anomalously large.

To study the behavior of the LDOS spectra as we go from a region of one gap size to another, we initially take a scan over a large area. Then we select several small areas and study them in detail, with a resolution of several spectra per atom. To maximize energy resolution, we limit the bias modulation used to acquire the dI/dV data to 2 mV, and apply minimal filtering for the data collection. Figure 2 shows maps of $\Delta(\vec{r})$ with a (a) small- and (b) large-gap region. Below each figure we also show line cuts of spectra along the arrow.

The spectra in Fig. 2(a) illustrate the evolution of the LDOS on going from a small-gap region with $\Delta < 30$ meV to an average-gap region with $\Delta_0 \sim 40$ meV. The crossover from one type of spectrum to the next occurs over a distance $\leq \xi_0$ with the anomalously large coherence peaks diminishing in strength while new peaks at the background

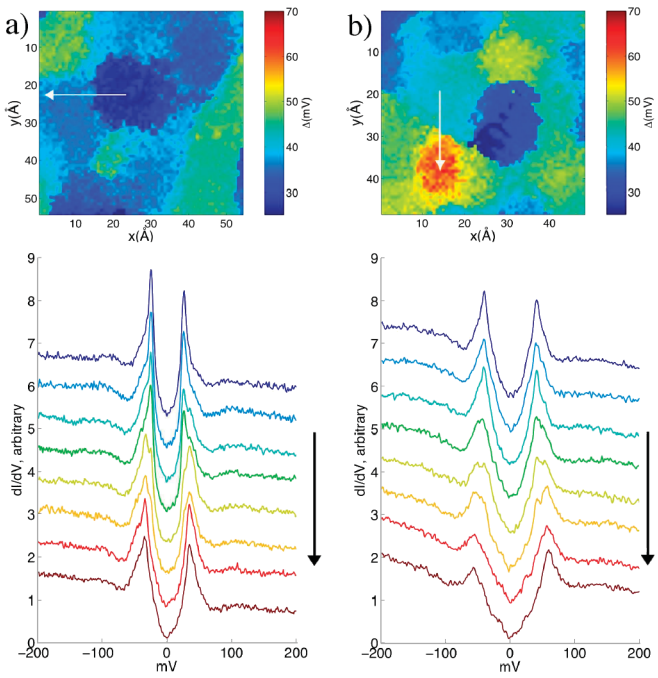

FIG. 2 (color). (a) Gap distribution and the evolution of spectra as this region is crossed near a (a) small-gap region and a (b) large-gap region. (Spectra follow arrows.)

gap of that region (typically $\sim\Delta_0$) increase in intensity. The signature at Δ_0 can be followed throughout the spectra from top (blue) to bottom (red): Deep in the small-gap region it appears as a weak shoulder above the main peak. At the border, a two-peak structure is apparent—one corresponding to the small-gap characteristics and the other near Δ_0. Finally, outside the small-gap region, the main peak occurs at about Δ_0 and has a more BCS-like structure. Line cuts through other small-gap regions show similar behavior, with the two-peak structure more visible when gap differences are large.

Figure 2(b) shows a line cut that starts in the average-gap region and ends up at the center of a large-gap region. Again, the peak corresponding to the average gap diminishes in strength without dispersing in energy, while a new broad peak appears at $\Delta \sim 65$ meV and the "average-gap" coherence peak becomes a shoulder inside the large gap. Other line cuts in different large-gap regions of the sample show similar evolution of the features, with the shoulder inside the gap being more or less visible when the differences in Δ are large/small.

Finally, as can be noted from Fig. 1 (inset), while small-gap regions may appear isolated in the background of the average gap, large-gap regions almost always appear within a distance $<\xi_0$ of small-gap regions. This feature may reflect the optimal-doping samples we are using, which favor the creation of small-gap regions.

To better understand these results, we computed the LDOS for a simple model, meant to represent an effective mean-field Hamiltonian for the quasiparticles:

$$\mathcal{H} = \sum_{\ell,\delta}\left[-t\psi_\ell^\dagger \tau_3 \psi_{\ell+\delta} + (-)^\delta \frac{\Delta(\ell)}{8}\psi_\ell^\dagger \tau_1 \psi_{\ell+\delta} + \text{H.c.}\right], \tag{1}$$

where the vectors ℓ label the lattice sites, δ are the nearest-neighbor vectors, and $(-)^\delta = 1$ for $\delta = \pm\hat{x}$ and $(-)^\delta = -1$ for $\delta = \pm\hat{y}$. In these expressions, we have adopted the usual Nambu notation with $\psi_\ell^\dagger = (c_{\ell\uparrow}^\dagger, c_{\ell\downarrow})$. In the uniform case, $\Delta(\ell) = \Delta_0$, $\mathcal{H}$ describes a uniform square lattice with near-neighbor hopping t and a d-wave mean field characterized by a gap $\Delta(k) = \frac{\Delta_0}{2}(\cos k_x - \cos k_y)$. In the following, we will consider the nonuniform situation in which $\Delta(\ell) = \Delta$ on the sites inside an $L \times L$ cluster embedded in a much larger ($M \times M$ with $M \gg L$) cluster in which $\Delta(\ell) = \Delta_0$. All the calculations shown in the present Letter are for $M = 800$ and $L = 5$, although we have performed calculations for a range of M's and confirmed that $M = 800$ is large enough that the results are independent of M.

We are interested in determining how the LDOS $N(\omega, \ell)$ varies as one moves from outside the cluster to sites inside the cluster, where

$$N(\omega, \ell) = N(\omega) - \frac{1}{\pi}\text{Im}\left[\sum_{\ell_1,\ell_2}{}' \text{Tr}[G(\ell - \ell_2)T(\ell_2, \ell_1)G(\ell_1 - \ell)]\right]. \tag{2}$$

Here $N(\omega)$ is the average density of states, $\sum'$ runs over sites inside the $L \times L$ patch, $G(\ell)$ is the single particle Green's function of the uniform lattice

$$G(\ell) = \frac{1}{N}\sum_k \left(\frac{\omega + \epsilon_k \tau_3 + \Delta_k \tau_1}{\omega^2 - \epsilon_k^2 - \Delta_k^2}\right) e^{ik\cdot\ell}, \tag{3}$$

and $T(\ell_2, \ell_1)$ is the T matrix associated with the scattering "potential" $\tilde{\Delta}(\ell) \equiv \Delta(\ell) - \Delta_0$,

$$T(\ell_2, \ell_1) = \sum_\delta (-)^\delta \frac{\tilde{\Delta}(\ell_2)}{8}\tau_1 \delta_{\ell_2, \ell_1 - \delta} + \sum_{\ell_3,\delta}{}' (-)^\delta \frac{\tilde{\Delta}(\ell_2)}{8}\tau_1 G(\ell_2 + \delta - \ell_3)T(\ell_3, \ell_1). \tag{4}$$

Representative results of our calculations are shown in Fig. 3 for $\Delta_0/t = 0.2$ and a small damping factor of 0.01. Results for the density of states at the center of a 5×5 cluster in which the gap amplitude in the cluster ranges from $\Delta = 2\Delta_0$ to $\Delta = 0$ are shown in Fig. 3(a). Here, one sees that when the gap amplitude in the cluster is large compared to the background, the density of states at the center of the patch has a broad response at $\omega = \pm\Delta$. However, as the cluster gap amplitude decreases below Δ_0, resonant peaks develop below $\pm\Delta_0$ and move down in energy as Δ decreases. The height of the resonance peaks also increases as Δ decreases. In order to illustrate the spatial dependence of $N(\omega, \ell)$, we consider the case in which $\Delta = 0$, corresponding to a zero pairing amplitude in the 5×5 patch. For this case, the density of states $N(\omega, \ell)$ versus ω for various sites (ℓ_x, ℓ_y) are shown in Fig. 3(b). Here, the site (0, 0) corresponds to the center of the cluster and results are shown for $\ell_y = 0$ with ℓ_x varying from 0 to 6. For sites inside the "gapless" cluster one sees a resonant response. This response appears at a lower energy than Δ_0 and the peak height, for a given broadening, is significantly larger than the logarithmic structure in the bulk d-wave density of states. As one moves out from the center of the cluster, the sharp low energy peak in the LDOS loses intensity and weight begins to grow at $\omega \sim \Delta_0$, so that at the boundary of the cluster a two-peak structure is clearly observed. Outside the cluster, the LDOS returns to its average behavior within a few lattice constants.

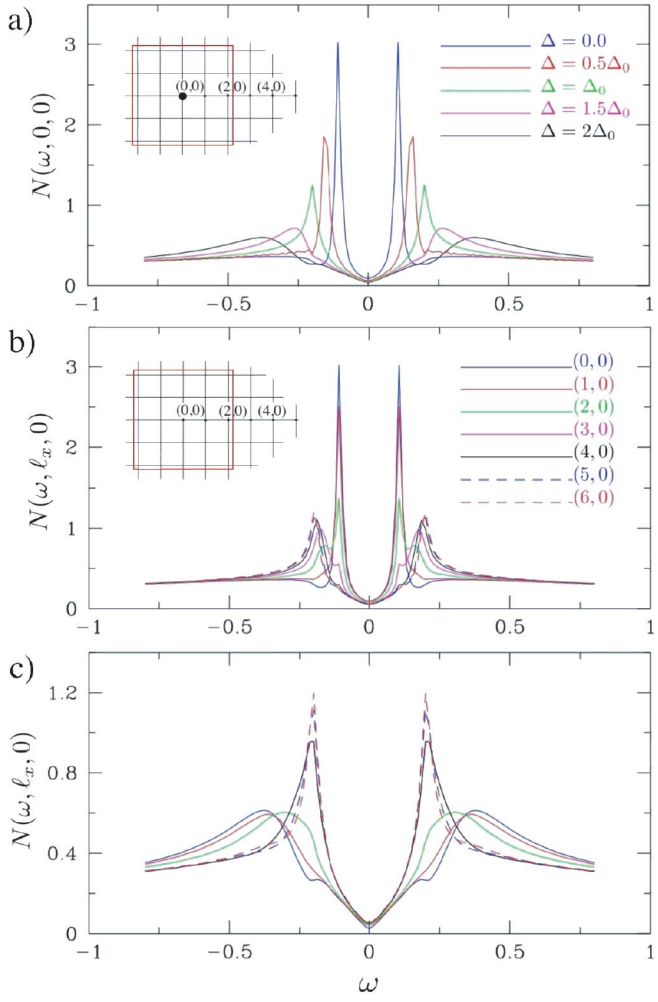

FIG. 3 (color). LDOS $N(\omega, \ell_x, \ell_y)$ versus ω for a 5×5 patch (outlined in red) centered at (0, 0). (a) LDOS at the center of the cluster $N(\omega, 0, 0)$ versus ω for different values of $\Delta(\ell)$. (b) $\Delta(\ell) = 0$ on the patch. (c) $\Delta(\ell) = 2\Delta_0$ on the patch and for both; $N(\omega, \ell_x, \ell_y)$ is shown for sites along $(\ell_x, 0)$.

If the gap parameter is doubled inside the cluster, $\Delta = 2\Delta_0$, one has $N(\omega, \ell)$ shown in Fig. 3(c). In this case, for

sites inside the cluster, $N(\omega, \ell)$ exhibits a broadened response near $2\Delta_0$ as well as a weak response at Δ_0. Here again, as one moves several lattice spacings outside the cluster, the density of states returns to its uniform behavior, characterized by the logarithmic coherence peaks at $\omega = \pm\Delta_0$. Note the change in scale between Figs. 3(a)–3(c) and how much stronger the resonance peaks are compared to the logarithmic peaks.

The low energy behavior of $N(\omega, \ell)$ is less dramatically ℓ dependent than the peak structure. Nonetheless, we believe that it is significant that the gap minimum is more v-shaped near the center of the large-gap cluster, and more rounded near the center of the small-gap cluster. We have not systematically explored the dependence of the results on the size of the cluster, L, but we have checked that similar behavior is obtained for somewhat different sized clusters and for clusters rotated by 45°.

The model we have solved is admittedly overly simple, especially in that it neglects the strong on-site Hubbard U. Nonetheless, the qualitative similarities between features of the model calculations and the STM data suggest that some aspects of the problem are being successfully modeled. Clearly there are structural variations from place to place in $Bi_2Sr_2CaCu_2O_{8+\delta}$; for instance, a positive correlation between the concentration of oxygen interstitials and the large-gap regions have been reported by McElroy *et al.* [10]. However, can structural differences due to these impurities give rise to a significant enhancement of the local pairing amplitude, and what about the regimes in which the gap is suppressed?

Rather, we propose that some type of intrinsic amplification of the effect of the structural variations is likely to be essential [19–21]. For instance, if (as has been previously suggested [19]) doped antiferromagnets are near the cusp of a first-order transition between two electronically distinct states, then small differences in the local structure can nucleate small regions of one phase or the other. It has been well established by now that above optimal doping ($x \approx 0.15$ holes per Cu atom in the Cu-O plane) the average gap decreases with increasing doping in proportion to T_c, roughly as $2\Delta \approx 8k_BT_c$. In underdoped samples, the average gap increases with decreasing doping, rising from $\Delta_0 \sim 40$ meV at optimal doping to $\Delta_0 \sim 55$ meV at around $x \approx 0.05$, where $T_c \to 0$ [22]. Correspondingly, STM studies of underdoped $Bi_2Sr_2CaCu_2O_{8+\delta}$ reveal that the fraction of large-gap regions increases with decreasing x, and the fraction of small-gap regions decreases [1,2,4]. Thus, it would be natural to identify the large-gap regions as being more representative of the electronic structure of underdoped cuprates and the small-gap regions more representative of overdoped cuprates, both influenced by some average-gap background. However, decreasing x also leads to a rapid decrease of T_c and the superfluid density, which implies that a large pairing field alone is insufficient to characterize the features of the electronic structure which reflect the approach to the Mott insulator.

A. C. F. and A. K. acknowledge support by DOE Grant No. DE-FG03-01ER45925. L. C. acknowledges support from NSF Grant No. Phy99-07949 at KITP (UCSB) where most of the reported calculations were carried out. L. C. and D. J. S. acknowledge useful discussions with L. Balents and support from NSF Grant No. DMR02-11166. S. K. acknowledges support from DOE Grant No. DE-FG03-00ER45798. Crystal growth was supported by DOE Grants No. DE-FG03-99ER45773 and No. DE-AC03-76SF00515.

*Present address: National Institute of Advanced Industrial Science and Technology, Tsukuba Central 2-2, Tsukuba, Ibaraki 305-8568, Japan.

[1] T. Cren *et al.*, Phys. Rev. Lett. **84**, 147 (2000).
[2] C. Howald, P. Fournier, and A. Kapitulnik, Phys. Rev. B **64**, 100504(R) (2001).
[3] S. H. Pan *et al.*, Nature (London) **413**, 282 (2001).
[4] K. M. Lang *et al.*, Nature (London) **415**, 412 (2002).
[5] A. Fang *et al.*, Phys. Rev. B **70**, 214514 (2004).
[6] A. Kapitulnik, A. Fang, C. Howald, and M. Greven, cond-mat/0407743 [J. Phys. Chem. Solids (to be published)].
[7] N. Momono, A. Hashimoto, Y. Kobatake, M. Oda, and M. Ido, J. Phys. Soc. Jpn. **74**, 2400 (2005).
[8] S. A. Kivelson *et al.*, Rev. Mod. Phys. **75**, 1201 (2003).
[9] C. Howald, H. Eisaki, N. Kaneko, and A. Kapitulnik, Proc. Natl. Acad. Sci. U.S.A. **100**, 9705 (2003); C. Howald *et al.*, Phys. Rev. B **67**, 014533 (2003).
[10] K. McElroy *et al.*, Phys. Rev. Lett. **94**, 197005 (2005).
[11] M. Vershinin *et al.*, Science **303**, 1995 (2004).
[12] Samples are prepared as slightly overdoped with $T_c \approx 89$ K. Cleaving at room temperature at UHV conditions may cause some oxygen to leave the exposed Bi-O surface layer yielding samples closer to optimal doping [2,13].
[13] M. Oda, C. Manabe, and M. Ido, Phys. Rev. B **53**, 2253 (1996).
[14] D. L. Feng *et al.*, Science **289**, 277 (2000).
[15] T. Valla *et al.*, Science **285**, 2110 (1999).
[16] Similar effects are seen in a self-consistent Bogoliubiv–de Gennes calculation for a model with a random dopant-modulated pairing interaction in T. S. Nunner, B. M. Andersen, A. Melikyan, and P. J. Hirschfeld, Phys. Rev. Lett. **95**, 177003 (2005).
[17] V. J. Emery and S. A. Kivelson, Nature (London) **374**, 434 (1995).
[18] C. Renner *et al.*, Physica (Amsterdam) **194B**, 1689 (1994).
[19] V. J. Emery, S. A. Kivelson, and H. Q. Lin, Phys. Rev. Lett. **64**, 475 (1990); S. A. Kivelson, G. Aeppli, and V. J. Emery, Proc. Natl. Acad. Sci. U.S.A. **98**, 11 903 (2001).
[20] P. W. Anderson *et al.*, J. Phys. Condens. Matter **16**, R755 (2004).
[21] A. Ghosal, A. Kopp, and S. Chakravarty, Phys. Rev. B **72**, 220502(R) (2005).
[22] See, e.g., the review by A. Damascelli, Z. Hussain, and Z-X. Shen, Rev. Mod. Phys. **75**, 473 (2003).